



Full length article

# Theoretical analysis of beam quality degradation in spectral beam combining of fiber laser array with beam deviation



Gang Bai<sup>a,b</sup>, Hui Shen<sup>a</sup>, Yifeng Yang<sup>a,\*</sup>, Xiang Zhao<sup>a,b</sup>, Jingpu Zhang<sup>a,b</sup>, Haibo Zhang<sup>a</sup>, Yunfeng Qi<sup>a,\*\*</sup>, Bing He<sup>a,c,\*\*\*</sup>, Jun Zhou<sup>a,d</sup>

<sup>a</sup> Shanghai Key Laboratory of All Solid-State Laser and Applied Techniques, Shanghai Institute of Optics and Fine Mechanics, Chinese Academy of Sciences, Shanghai 201800, China

<sup>b</sup> University of Chinese Academy of Sciences, Beijing 100049, China

<sup>c</sup> Nanjing Institute of Advanced Laser Technology, Nanjing, Jiangsu 210038, China

<sup>d</sup> Nanjing Zhongke Shengguang Technology Co., Ltd, Nanjing, Jiangsu 210038, China

## ARTICLE INFO

### Article history:

Received 9 October 2017

Received in revised form 18 January 2018

Accepted 12 March 2018

### Keywords:

Spectral beam combining

Fiber laser array

Beam deviation

Beam quality

## ABSTRACT

Aimed to maintain excellent beam quality, the degradation of  $M^2$  factor is theoretically studied in compact spectral beam combining (SBC) system of fiber laser array. Considering that the output beams from a laser array usually have axial translation and angular deflection, the correction of incident light field is built by the transformation of coordinates. Using the propagation model and the statistics, properties of the combined beam with perturbations of a single emitter or entire laser array are respectively discussed in detail. The degradation of  $M^2$  factor is  $0.14(\pm 0.075)$  when the axial translation of entire laser array satisfies normal distribution with standard deviation of  $100\ \mu\text{m}$ . While the angular deflection is introduced with standard deviation of  $10/3\ \text{mrad}$ , the degradation increases to  $3.57(\pm 1.28)$ . Owing to non-overlap ensemble of the incident beam on the grating, the deflection angle will translate the far-field beam spot after the diffraction, which causes a dramatic degradation of the beam quality. Considering the axial translation and the angular deflection simultaneously, the overall effect on the beam quality is dominated by the angular deflection. For applicable requirements of  $M^2 < 2, 3\ \text{mrad}$  angular deflection is claimed with axial translation less than  $300\ \mu\text{m}$  in the compact SBC system. These analyses provide a valid basis for building the experimental system of SBC.

© 2018 Elsevier Ltd. All rights reserved.

## 1. Introduction

High-brightness beam combining of fiber lasers provides a path for power scaling beyond the single fiber limit while maintaining many of the benefits of fiber lasers. Compared with coherent combining, incoherent spectral beam combining (SBC) have the advantages of permitting independent modulation of the lasers, not requiring phase control and interferometric alignment tolerances [1–3]. Beams with diverse wavelength in SBC are overlapped in both the near and far fields to achieve high concentration of power with near-diffraction limited output beam. In 2000, Daneu et al. proposed the SBC of a laser array in the external resonator config-

uration, achieving a SBC of 11-channel, wideband diode array, obtaining 20 times diffraction limit output [4]. This technique is also widely used in the fiber laser to increase laser brightness. The combined output power of SBC increases from 522 W to 8.2 kW with the beam quality degradation from 1.22 to 4.3 [5,6]. With the expansion of the laser array scale, Lockheed Martin Inc. has achieved a breakthrough in the total power of SBC from 3 kW to 30 kW with a beam quality of  $M_x^2 = 1.6$  and  $M_y^2 = 1.8$  [7,8].

The output power of SBC is determined by the number of emitters and power of a single laser, while the beam quality of the combined beam is theoretically identical to that of the individual beam from a single emitter. However, the beam quality is susceptible to the thermal distortion of diffraction grating, the optical aberration of transform lens, and beam deviation of laser arrays. According to a propagation model based on multilayer dielectric gratings (MDGs) [9–12], the combined beam quality degrades with the parameters and fabrication errors of MDGs [9,10] and aberration coefficient of the transform lens [11]. In these analyses, an ideal laser array is assumed, but the beam deviation of misaligned laser array also influences the properties of the combined beam,

\* Corresponding author.

\*\* Corresponding author.

\*\*\* Corresponding author at: Shanghai Key Laboratory of All Solid-State Laser and Applied Techniques, Shanghai Institute of Optics and Fine Mechanics, Chinese Academy of Sciences, Shanghai 201800, China.

E-mail addresses: [yf\\_cumt@126.com](mailto:yf_cumt@126.com) (Y. Yang), [dreamer\\_7@siom.ac.cn](mailto:dreamer_7@siom.ac.cn) (Y. Qi), [bryanho@siom.ac.cn](mailto:bryanho@siom.ac.cn) (B. He).

especially the beam quality, which has been a key performance index for evaluating the effect of the high-energy laser. For the wideband diode array, the non-ideal “smile” effect on the combined beam quality has been investigated using the ray-tracing method [12]. However, due to the different divergence angles in two orthogonal directions, diode laser arrays of SBC require complex beam shaping system with the output field of super-Gaussian distribution. The order of the super-Gaussian is hard to be determined precisely and the initial beam quality is unknown which reduces the usefulness and effectiveness of simulation. In contrast, the fiber laser array where the emitters release nearly diffraction-limited Gaussian beams is more applicable to establish SBC model for simulating and optimizing the beam quality. Most importantly, as the multiple beam combination with stochastic beam deviation, a systematical statistical analysis is critical for evaluating the beam quality precisely. For the numerical calculation, compared with the ray-tracing method, the approach using rigorous coupled wave analysis is stricter to consider phase modulation on the MDG in subwavelength structures (grating constant  $d \approx \lambda$ ) [13]. To our best knowledge, the influence of beam deviation on the fiber SBC architecture is rarely analyzed in previous reports.

In this paper, the combined beam quality of SBC has been chosen as a universal standard to evaluate the changes caused by

external disturbances that surround emitters, such as fabrication errors, mechanical vibration and temperature change. The paper is organized as follows. In Section 2, the incident light fields of beams with axial translation and angular deflection are derived by the transformation of coordinates and pass through the compact SBC system based on the beam propagation model. The intensity distributions and  $M^2$  factor of the combined diffraction beams are numerically calculated and analyzed in mathematical statistics in Section 3. Conclusions are drawn in Section 4. We believe that this reliable analysis will play an important role in establishing SBC system of fiber lasers in practice.

### 2. Theoretical model

A schematic diagram for SBC system is shown in Fig. 1(a), consisting of fiber laser array, a transform lens, and a diffraction grating. The transform lens is located between the laser array and MDG to ensure that each individual beam is collimated and spatially overlapped on the MDG. All beams with different wavelengths whose incident angles specially satisfy the grating equation can be exported along the common aperture. Therefore, the emission wavelength of each beam is determined by both the MDG and the position of laser emitter. Compared with free propagation of

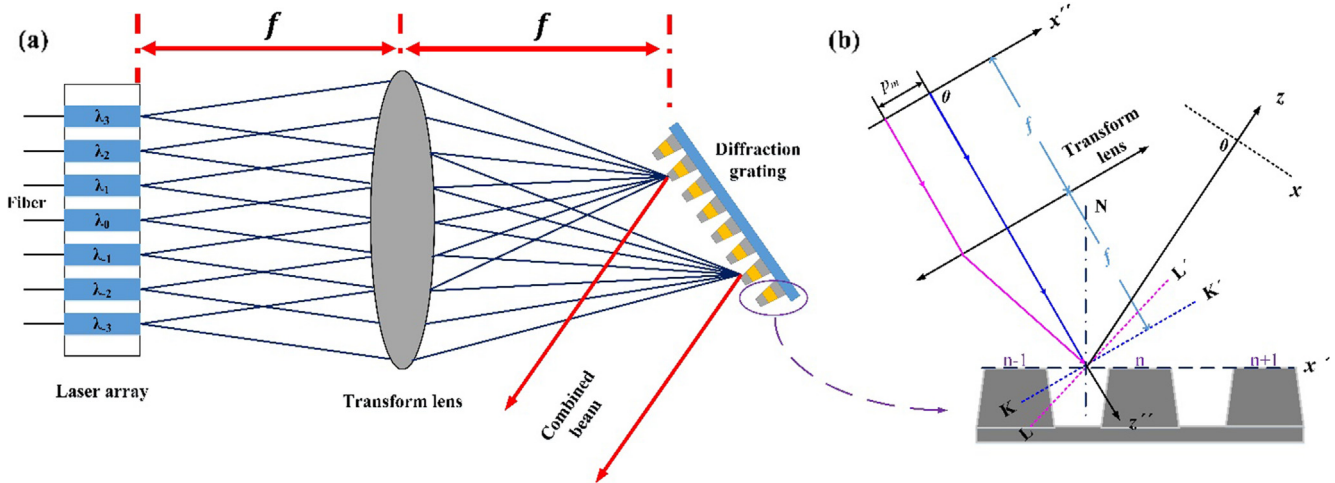


Fig. 1. (a) Schematic illustration and (b) simplified mathematical model of SBC system.  $LL'$  and  $KK'$  are equiphase surface for the different sub-beam;  $n$ , the numerical order of the relief.

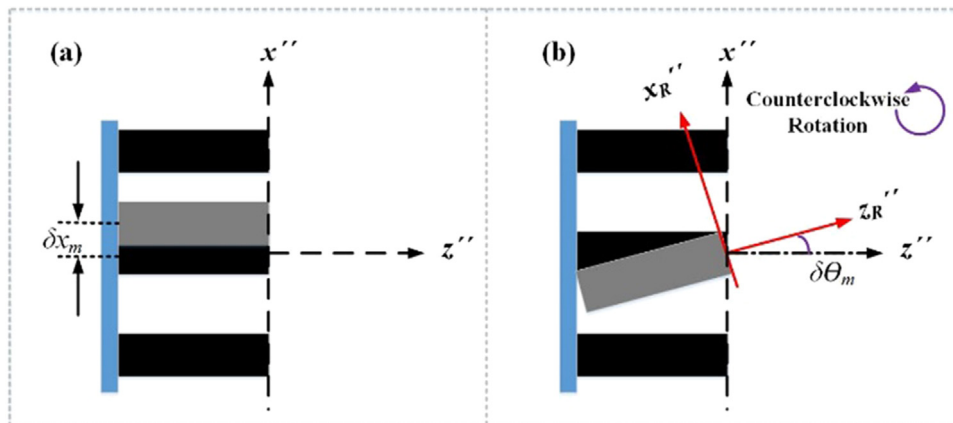


Fig. 2. Beam deviation of emitters including: (a) axial translation with  $\delta x_m$ ; (b) angular deflection with  $\delta \theta_m$ .

the laser array, the configuration ensures that the combined beam has superior beam quality and higher power.

### 2.1. Beam propagation model of SBC system

The simulation for SBC is divided into the following steps: (i) each individual beam emitted from the fiber laser array is converged on the grating by the transform lens. (ii) All of the incident beams meeting a one-to-one relationship between wavelengths and incidence angles are collimated after the diffraction of the MDG. (iii) All of the diffraction beams in a common aperture are

**Table 1**

Parameters used for simulations of compact SBC system.

Parameter	Value	Parameter	Value
$w_0$ ( $\mu\text{m}$ )	300	$\lambda_0$ (nm)	1064
$\Delta p$ (mm)	5	$\alpha_0$ (degree)	36.25
$f$ (mm)	300	Axial translation range ( $\mu\text{m}$ )	30–300
Grating constant $d$ (mm)	1/960	Angular deflection range (mrad)	1–10
Diffraction order $q$	1		

superposed incoherently after the grating. As shown in Fig. 1(b), two Cartesian coordinate systems are established for the incident and diffraction beams, respectively. In the incident coordinate system,  $2M + 1$  fiber lasers located in the focal plane of the lens ( $x''$  axis) are symmetrically arranged along the optical axis of the lens ( $z''$  axis). For the diffraction one,  $z$  axis is set along the combined diffraction beams, and the  $x$  axis on the observing plane is perpendicular to that. A reference plane set as  $x'$  axis is used to describe the incident field distribution at the surface of the MDG. The displacement between the  $m$ th laser center and the zero point is  $p_m = m\Delta p$ , where  $\Delta p$  is the spacing of adjacent fiber lasers.

Assuming that each individual laser is approximately a fundamental Gaussian beam with beam waist width  $w_0$ , the field distribution of the  $m$ th individual beam can be written as

$$E_m(x_0, 0) = E_0 \exp \left[ -\frac{(x_0 - p_m)^2}{w_0^2} \right], \quad (1)$$

where  $E_0$  is the central amplitude of the incident beam. The propagation matrix between the laser array and the MDG is

$$\begin{pmatrix} A & B \\ C & D \end{pmatrix} = \begin{pmatrix} 1 & z'' - f \\ 0 & 1 \end{pmatrix} \begin{pmatrix} 1 & 0 \\ -\frac{1}{f} & 1 \end{pmatrix} \begin{pmatrix} 1 & f \\ 0 & 1 \end{pmatrix}, \quad (2)$$

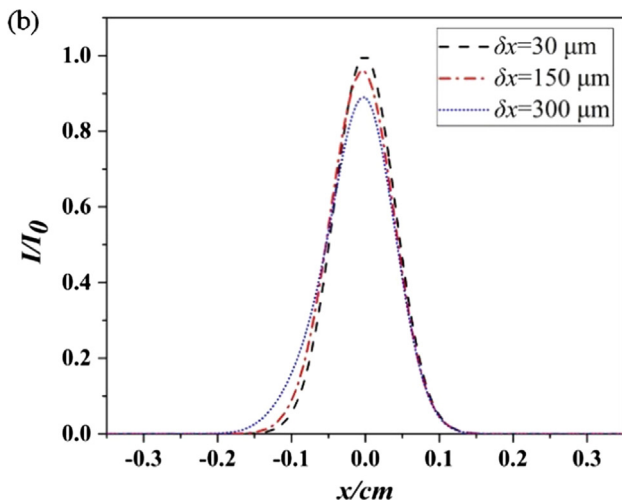
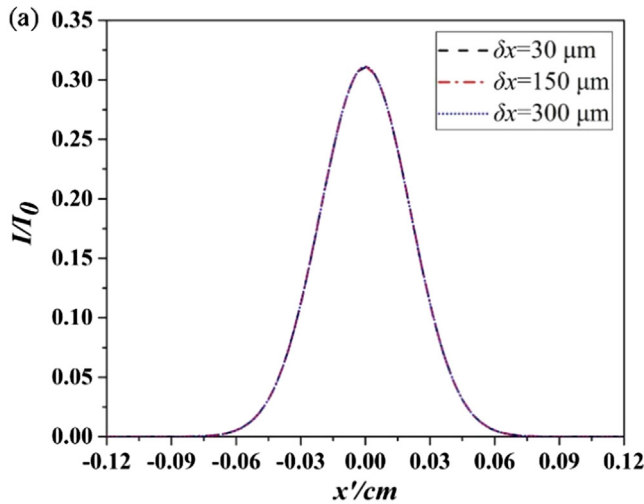


**Fig. 3.** The normalized intensity distribution when a single emitter has axial translation in the fiber laser array: (a) the incident light field of the perturbed emitter before the diffraction; (b) the combined light field after the MDG at  $z = 1$  m.  $I_0$  is maximum intensity of the combined beam corresponding to  $\delta x = 30 \mu\text{m}$ .

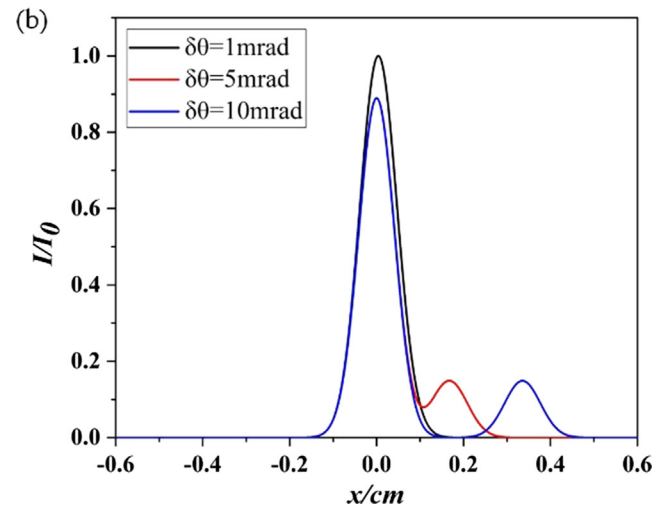
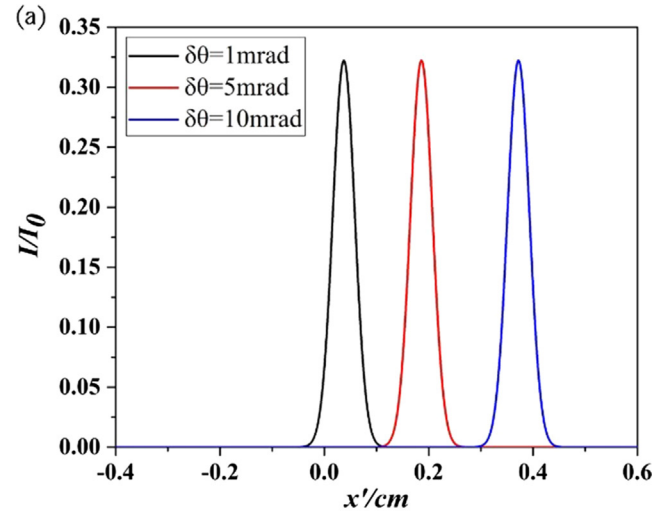


**Fig. 4.** The normalized intensity distribution when a single emitter has deflection angle in the fiber laser array: (a) the incident light field of the perturbed emitter before the MDG; (b) the combined light field after the MDG at  $z = 1$  m.  $I_0$  is maximum intensity of the combined beam corresponding to  $\delta\theta = 1$  mrad.

where  $f$  is the focal length of the transform lens:  $f > 0$  is the convex lens;  $f < 0$  is the concave lens.

When the beam propagates through the transform lens, the field distribution of the beam on the incident plane of the grating can be calculated by utilizing the Collins diffraction integral [14,15]

$$E_m(x'', z'') = \sqrt{\frac{1}{i\lambda_m B}} \exp(ik_m z'') \int_{-\infty}^{+\infty} E_m(x_0, 0) \times \exp\left[\frac{ik_m}{2B}(Ax_0^2 - 2x_0 x'' + Dx''^2)\right] dx_0, \quad (3)$$

where  $k_m = 2\pi/\lambda_m$ ,  $\lambda_m$  is the wavelength of the  $m$ th emitter;  $A, B, C$  and  $D$  can be obtained by calculating the propagation matrix. Providing that the complex amplitude in one grating period remains constant [16], the incident field on the MDG is determined by the numerical order of the relief  $n$  only and can be recorded as  $E_m(n)$ .

According to scalar diffraction theory [17], the diffraction field of the  $m$ th emitter after the MDG can be expressed as

$$E_m(x, z) = F^{-1}[F(E_m(n) * \exp(i\phi)) * H(f_x, z)], \quad (4)$$

$$H(f_x) = e^{ikz} \exp[-j\pi\lambda z f_x^2], \quad (5)$$

where is the near-field phase modulation on the MDG. As subject to the rigorous coupled wave analysis [13], the near-field equiphase surface is a plane without thermal deformation on the MDG ( $\phi$  is a constant).  $F$  is Fourier transform,  $F^{-1}$  is inverse Fourier transform,  $z$  is observed distance, and  $f_x$  is spatial frequency along the  $x$  axis. By the principle of incoherent superposition, the far-field intensity distribution of the combined beam can be expressed as

$$I(x, z) = \sum_{m=-M}^M |E_m(x, z)|^2.$$

The  $M^2$  factor of the combined beam on the  $x$  axis can be calculated using the intensity second-order moment method [18]. This method fits the curve of the squared beam radius  $w^2$  of the combined beam against the propagation distance  $z$ . The  $M^2$  factor of the combined beam can be calculated from

$$w^2(z) = az^2 + bz + c, \quad M^2 = \frac{\pi}{\lambda} \sqrt{ac - \frac{b^2}{4}}, \quad (6)$$

where parameter  $a, b$  and  $c$  are obtained by the corresponding polynomial fitting coefficients.

### 2.2. Model of fiber laser array with beam deviation

The fiber laser array is not perfectly aligned due to fabrication tolerance, accuracy of artificial adjustment, ambient vibration and so on. As illustrated in Fig. 2(a), the incident light field with an axial translation  $\delta x_m$  can be corrected as

$$E_m(x_0, 0) = E_0 \exp\left[-\frac{(x_0 - p_m - \delta x_m)^2}{w_0^2}\right]. \quad (7)$$

When the emitters rotate around the output end with the angle of  $\delta\theta_m$  in Fig. 2(b), the amplitude of the output field is still Gaussian distribution  $E_m(x''_R, 0) = E_0 \exp\left[-\frac{(x''_R - p_m \cos \delta\theta_m)^2}{w_0^2}\right]$  in the new coordinate system with  $z''_R$  axis along the direction of the beam. The rotated light field is rewrite in the coordinate system  $x''oz''$  by the transformation of coordinates, which is expressed as

$$\begin{bmatrix} x''_R \\ z''_R \end{bmatrix} = \begin{bmatrix} \cos \delta\theta_m & -\sin \delta\theta_m \\ \sin \delta\theta_m & \cos \delta\theta_m \end{bmatrix} \begin{bmatrix} x'' \\ z'' \end{bmatrix}. \quad (8)$$

The light field of one beam with angular deflection is

$$E_m(x_0, 0) = E_0 \exp\left\{-\frac{[(x_0 - p_m) \cos \delta\theta_m]^2}{w_0^2}\right\} \times \exp[ik(x_0 - p_m) \sin \delta\theta_m], \quad (9)$$

where the phase term is induced by the extra optical path respective to the reference phase plane  $z'' = 0$  after the rotation. Submitting Eqs. (7) and (9) to Eq. (3), the incident field on the MDG is derived for calculating the diffracted field and beam quality. In the following, the perturbations of beam deviation on a single emitter and the entire array are analyzed in detail.

### 3. Simulations and results

Based on the discussion presented above, the corresponding numerical algorithm is built up. For simplicity and without loss of generality, a laser array consisting of seven individual emitters are adopted in the SBC system (Fig. 1).

The wavelength interval of two adjacent lasers will be determined by differential operation of the grating equation  $\Delta\lambda = \Delta p \cdot d \cos \alpha_0 / (qf)$  [19]. All parameters employed in the numerical simulations are listed in Table. 1.  $\lambda_0$  is the wavelength

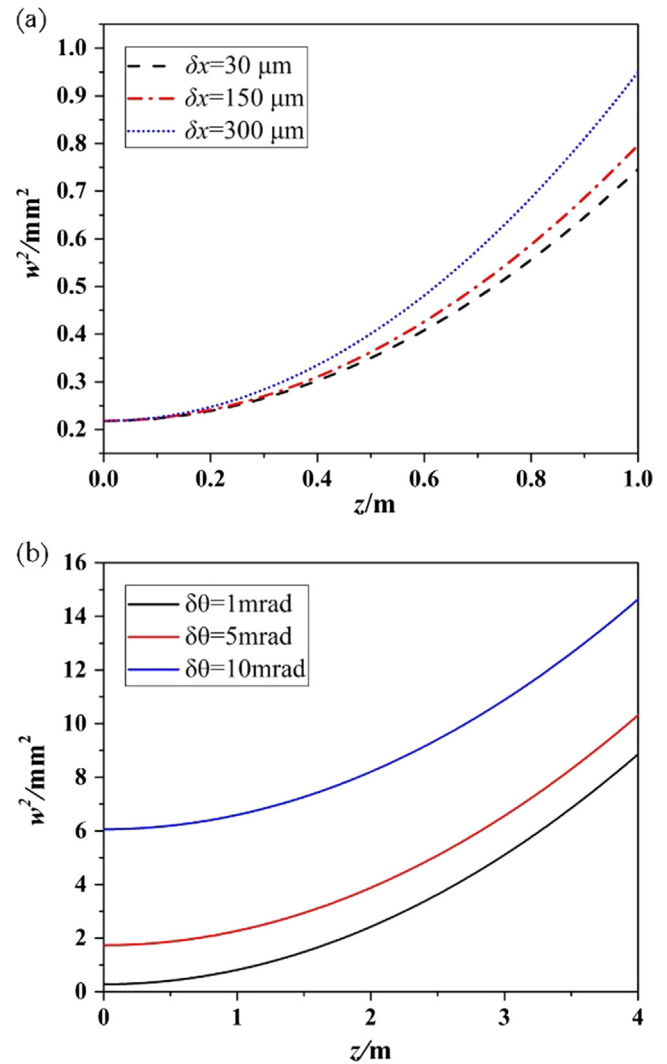


Fig. 5. Squared of beams radius for different propagation distances with (a) axial translations and (b) angular deflections of a single fiber laser.

of central emitter at the zero point ( $m = 0$ ), and  $\alpha_0$  is the incident angle of the beam relative to grating normal.

3.1. Single emitter with axial translation and angular deflection

In this section, the central position of fiber laser array ( $m = 0$ ) is used as perturbation source, occurring quantitative axial translation and deflection angle, respectively. The surface of the grating is used as a reference plane to describe the incident field distribution of single perturbed emitter. The diffracted field of entire array comes along the  $z$  axis, which is an important complement to the numerical change of beam quality. We take the typical values 30  $\mu\text{m}$ , 150  $\mu\text{m}$ , 300  $\mu\text{m}$  as the axial translation and 1 mrad, 5 mrad, 10 mrad as deflection angle, referring to precision industrial processing standards.

Fig. 3(a) gives the intensity distribution of the emitter with axial translation before the diffraction. All of the field distributions are spatially overlapped completely at the surface of the grating for

three different translations. However, the axial translation before the transform lens can induce the change of angles incident on the MDG. As a result, the one-to-one relationship meeting grating equation between the wavelength and angle of the incident laser is destroyed. Therefore, the far-field intensity distributions of the combining beams shown in Fig. 3(b) extend slightly along the transverse ( $x$  axis).

Fig. 4 gives the intensity distributions of the perturbed emitter with angular deflection. Differing from the axial translation in Fig. 3(a), the intensity distribution of the perturbed light field (Fig. 4(a)) is shifted and the incident light fields do not satisfy the common aperture condition (spatially overlapped) at the surface of the MDG. The combined far-field intensity distribution is distorted or even split inevitably due to the incident position deviation caused by angular deflection, shown in Fig. 4(b). However, the discussion of the field distribution at a single location cannot quantify the change of beam quality, which is resolved through iterations of this process at each location.

**Table 2**  
Beam quality of the combined beams with the disturbance of a single emitter.

Beam deviation	Axial translations $\delta x_m$ ( $\mu\text{m}$ )			Angular deflections $\delta \theta_m$ (mrad)		
	30	150	300	1	5	10
$M^2$ Factor	1.01	1.05	1.18	1.15	2.85	5.33

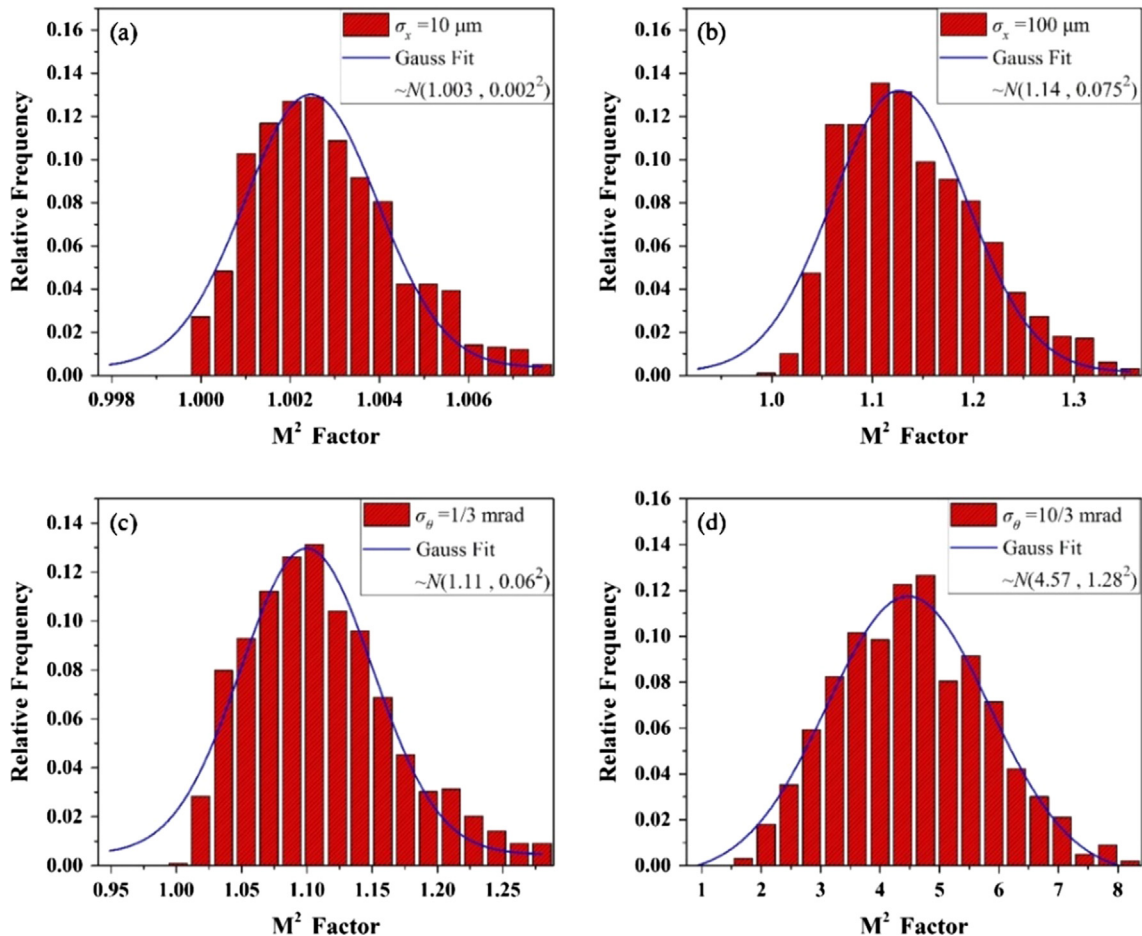


**Fig. 6.** Beam quality  $M^2$  factor of combined beams with random perturbation of fiber laser array: (a)  $\sigma_x = 10 \mu\text{m}$ ,  $M^2 = (1.003 \pm 0.002)$ ; (b)  $\sigma_x = 100 \mu\text{m}$ ,  $M^2 = (1.14 \pm 0.075)$ ; (c)  $\sigma_\theta = 1/3 \text{ mrad}$ ,  $M^2 = (1.11 \pm 0.06)$ ; (d)  $\sigma_\theta = 10/3 \text{ mrad}$ ,  $M^2 = (4.57 \pm 1.28)$ .

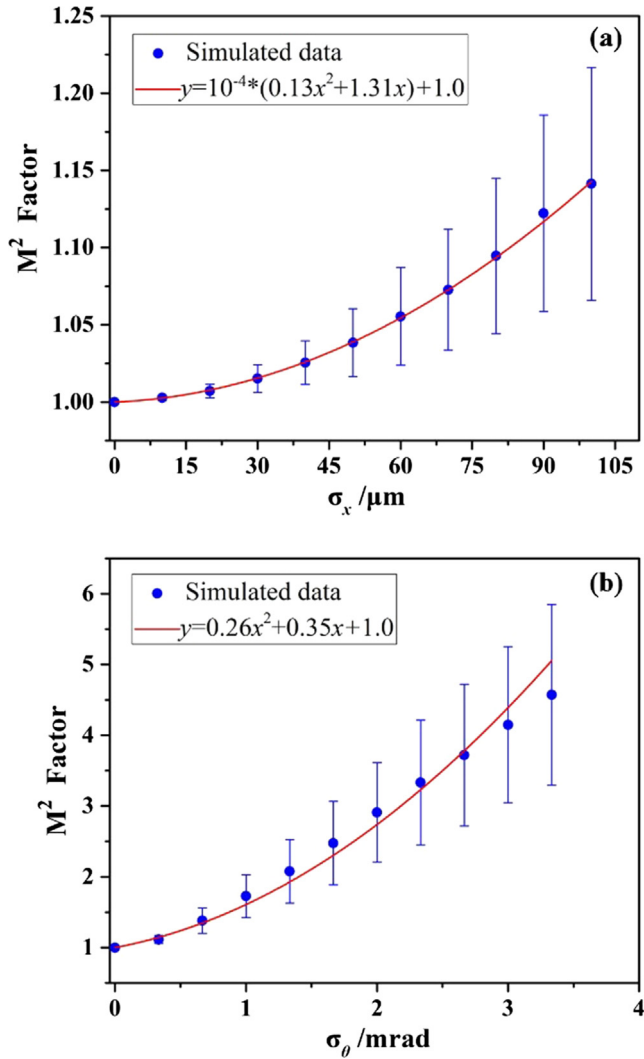


Fig. 7. The statistical results of the  $M^2$  factor with different beam deviations: (a) axial translation with  $\sigma_x$ ; (b) angular deflection with  $\sigma_\theta$ .

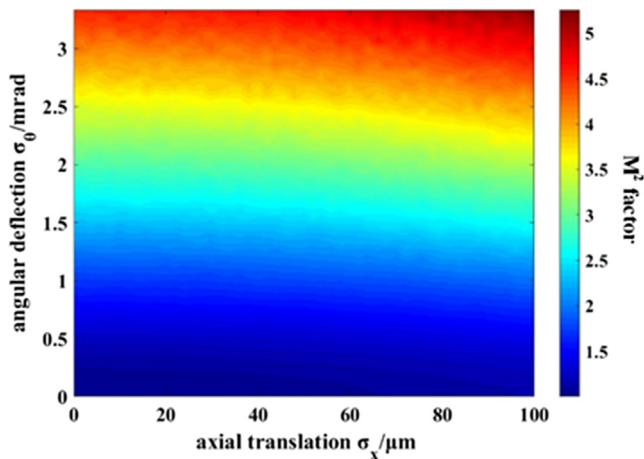


Fig. 8. The beam quality versus axial translation  $\sigma_x$  and angular deflection  $\sigma_\theta$ .

The squared beam radius  $w^2$  obtained for the combined beam under different  $z$  is investigated in Fig. 5. Comparing with Fig. 5 (b), the axial translation does not increase the beam radius at the initial position ( $z = 0$ ) in Fig. 5(a), which is consistent with the

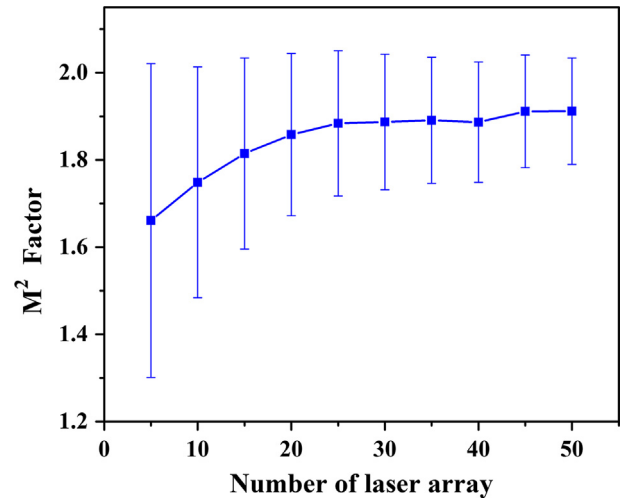


Fig. 9. The variation tendency of statistical  $M^2$  factor with the expansion of the scale of laser array ( $\sigma_0 = 1$  mrad).

above common aperture condition. The  $M^2$  factors of the combined beam with different beam deviation are given in Table 2, which are calculated using Eq. (6). When the deflection angle increases from 1 mrad to 10 mrad, the combined beam quality is degraded from 1.15 to 5.33. The changes of  $M^2$  factor are more sensitive to the angular deviation.

### 3.2. Evaluating $M^2$ factor with random perturbation of entire laser array

The previous comments focus on the case where a single emitter is misaligned with axial translation and angular deflection. In practice, for the entire laser array the combined beam quality can be affected by many error sources, such as fabrication tolerance, accuracy of artificial adjustment and ambient vibration. Due to the randomness of these sources for all emitters, the degradation of beam quality should be analyzed statistically. A large number of independent random events tend towards a normal distribution according to the center limit theorem in probability and statistical theory [20]. Therefore, beam deviation of misaligned laser array spreads as a normal distribution with probability density function (PDF)

$$f(i) = \frac{1}{\sqrt{2\pi}\sigma_i} \exp\left(-\frac{(i - \mu_i)^2}{2\sigma_i^2}\right) \sim N(\mu_i, \sigma_i^2), \quad (10)$$

where  $i = x, \theta$  for the axial translation and angular deflection, respectively.  $\mu_i$  denotes the mean;  $\sigma_i$  is the standard deviation. About 99.7% of values drawn from a normal distribution are within  $3\sigma_i$  away from  $\mu_i$ . The mean of beam deviation is equal to zero for the independent and identically distributed random variables. Consequently, the disturbance ( $\delta x_m$  and  $\delta \theta_m$ ) of entire laser array can be considered to locate in the interval  $[-3\sigma_i, 3\sigma_i]$ , and thus the maximum random perturbation is equal to  $\pm 3\sigma_i$ .

The  $M^2$  factor is calculated for the standard deviation of axial translation and angular deflection in the interval  $[10 \mu\text{m}, 100 \mu\text{m}]$  and  $[1/3 \text{ mrad}, 10/3 \text{ mrad}]$ . This simulation is repeated 1000 times for rational statistical regularity and  $M^2$  values is divided into 20 samples of sizes uniformly for counting as relative frequency. The density-scaled histograms of probability distribution for  $M^2$  factor are shown in Fig. 6 with samples of the maximum and minimum standard deviation. The statistical  $M^2$  factor agrees to the normal distribution. The degeneration of beam quality caused by the beam deviation is compared with the beam quality

of fundamental Gaussian beam, whose beam quality factor is  $M^2 = 1$ . The degradation of beam quality for the axial translation is respectively  $0.003(\pm 0.002)$  and  $0.14(\pm 0.075)$  for the standard deviation of  $10\ \mu\text{m}$  and  $100\ \mu\text{m}$  in Fig. 6(a) and (b), for the angular deflection  $0.11(\pm 0.06)$  and  $3.57(\pm 1.28)$  corresponding to  $1/3$  mrad and  $10/3$  mrad in Fig. 6(c) and (d).

Fig. 7 shows the trend of  $M^2$  factor versus the standard deviation of beam deviation. The mean and standard deviation of  $M^2$  factor is increasing gradually with the perturbation parameter ( $\sigma_x$  and  $\sigma_\theta$ ) in both cases. Second order polynomials are used to fit  $M^2$  factors. For the axial translation  $M_x^2 = 10^{-4} * (0.13\sigma_x^2 + 1.31\sigma_x) + 1.0$  and the angular deflection is  $M_\theta^2 = 0.26\sigma_\theta^2 + 0.35\sigma_\theta + 1.0$ .

However, the axial translation and angular deflection are always linked with each other in reality, and the overall effects of beam deviation on the output beam quality are shown in Fig. 8. Comparing with angular deviation, the axial translation has slight impact on the beam quality within a larger range  $0\text{--}100\ \mu\text{m}$  of standard deviation. Therefore, angular deviation is concerned more for an actual SBC system. When the standard deviation of the axial translation is within  $100\ \mu\text{m}$  which is a large fabrication error, the empirical function for angular deviation (red<sup>1</sup> line in Fig. 7(b)) can be employed to evaluate the change of combined beam quality  $M^2$  factor. In the design of a SBC system, we need to pay more attention to the angular deflection, and restrict errors in axial and angular deviation of all beams according to the specific beam quality requirements. For an excellent beam quality of 2, the maximum deflection angle has to be controlled under  $3$  mrad in the compact SBC system.

For achieving the brightness scaling of combined beam, it is necessary to further evaluate the continuous variation of the combined beam quality as the increase of individual emitters. A laser array including 50 emitters is calculated to estimate the variation of beam quality with a fixed deflection angle. The standard deviation of  $1$  mrad is chosen as the disturbance variable along with the continuous expansion of laser array. As shown in Fig. 9, when the number of emitters is less than 25, the mean of  $M^2$  factor increases slowly, and tends to be stable ( $M^2 = 1.9$ ) as that exceeds 25. The standard deviation gradually decreases and approaches a constant  $\sim 0.13$ . It is implied that the influence of angular deviation on the beam quality will not continue to deteriorate and gradually become constant with the scale expansion of the laser array.

#### 4. Conclusion

In summary, we develop the propagation model of SBC systems and further apply it to conduct statistical evaluation of fiber laser array with beam deviation, which consists of axial translation and angular deflection in fact. The incident light fields of beams with pointing deviation are derived by the transformation of coordinates. On the basis, the degradation of  $M^2$  factors affected by parameters of misaligned fiber laser arrays are discussed in mathematical statistics. The simulation indicates that the  $M^2$  factor of the combined beam degrades obviously when considering the deflection angles of emitters, whereas the axial translation has slight impact on the intensity distribution and the beam quality of the combined beam. It can be distinguished whether the common aperture condition is destroyed at the incident plane of the MDG (Figs. 3(a) and 4(a)). Considering the axial translation and the angular deflection simultaneously, the overall effect of beam deviation indicates that the degradation of combined beam quality is dominated by the angular deflection, which can be fitted by simple function  $M_\theta^2 = 0.26\sigma_\theta^2 + 0.35\sigma_\theta + 1.0$ . For achieving beam

quality of 2, the deflection angle expects less than  $3$  mrad even though the axial translation is up to  $300\ \mu\text{m}$  corresponding to the standard deviation of  $100\ \mu\text{m}$  in the compact SBC system. Moreover, the effect of angular deviation on the beam quality will not continue to deteriorate and gradually become constant with the scale expansion of the laser array. These analyses will be beneficial to optimize the SBC system for higher power and better beam quality output.

#### Acknowledgement

This research is sponsored by the National Natural Science Foundation of China (61405202, 61705243), National Science Foundation of Shanghai (16ZR1440100, 16ZR1440200), Program of Shanghai Technology Research Leader (17XD1424800), Shanghai Sailing Program (17YF1421200), the key technologies R&D program of Jiangsu (BE2016005-4), and K.C.Wong Education Foundation.

#### References

- [1] S. Klingebiel, F. Röser, B. Ortaç, J. Limpert, A. Tünnermann, Spectral beam combining of Yb-doped fiber lasers with high efficiency, *J. Opt. Soc. Am. B* 24 (2007) 1716–1720.
- [2] T.H. Loftus, A.M. Thomas, P.R. Hoffman, M. Norsen, R. Royse, A. Liu, E.C. Honea, Spectrally beam-combined fiber lasers for high-average-power applications, *IEEE J. Sel. Top. Quantum Electron.* 13 (2007) 487–497.
- [3] T. Schreiber, C. Wirth, O. Schmidt, V. Thomas, S. Andersen, T. Böhme, F. Peschel, T. Brückner, F. Röser Clausnitzer, R. Eberhardt, J. Limpert, A. Tünnermann, Incoherent beam combining of continuous-wave and pulsed Yb-doped fiber amplifiers, *IEEE J. Sel. Top. Quantum Electron.* 15 (2009) 354–360.
- [4] V. Daneu, A. Sanchez, T.Y. Fan, H.K. Choi, C.C. Cook, Spectral beam combining of a broad-stripe diode laser array in an external cavity, *Opt. Lett.* 25 (2000) 405–407.
- [5] T.H. Loftus, A. Liu, P.R. Hoffman, A.M. Thomas, M. Norsen, R. Royse, E. Honea, 522 W average power, spectrally beam-combined fiber laser with near-diffraction-limited beam quality, *Opt. Lett.* 32 (2007) 349–351.
- [6] C. Wirth, O. Schmidt, I. Tsybin, T. Schreiber, R. Eberhardt, J. Limpert, A. Tünnermann, K. Ludewigt, M. Gowin, E. Have, M. Jung, High average power spectral beam combining of four fiber amplifiers to 8.2 kW, *Opt. Lett.* 36 (2011) 3118–3120.
- [7] Eric Honea, Robert S. Afzal, Matthias Savage-Leuchs, Neil Gitkind, Richard Humphreys, Jason Hentie, Khush Brar, Don Jander, Spectrally beam combined fiber lasers for high power, efficiency and brightness, *SPIE* 8601 (2013) 860115.
- [8] Eric Honea, Robert S. Afzal, Matthias Savage-Leuchs, Jason Hentie, Khush Brar, Nathan Kurz, Don Jander, Neil Gitkind, Hu. Dan, Craig Robin, Andrew M. Jones, Ravi Kasinadhuni, Richard Humphreys, Advances in fiber laser spectral beam combining for power scaling, *SPIE* 9730 (2015) 97300Y.
- [9] Z. Wu, Z. Zhong, L. Yang, B. Zhang, Beam properties in a spectral beam combining system based on trapezoidal multilayer dielectric gratings, *J. Opt. Soc. Am. B* 33 (2016) 171–179.
- [10] L. Yang, Z. Wu, B. Zhang, Influence of thermal deformation of a multilayer dielectric grating on a spectrally combined beam, *Appl. Opt.* 55 (2016) 9091–9100.
- [11] Y. Zhang, B. Zhang, Analysis of beam quality for the laser beams after spectral beam combining, *Optik* 121 (2010) 1236–1242.
- [12] Z. Wu, L. Yang, Z. Zhong, B. Zhang, Influence of laser array performance on spectrally combined beam, *J. Mod. Opt.* 63 (2016) 1972–1980.
- [13] L. Li, Y. Jin, F. Kong, L. Wang, J. Chen, J. Shao, Beam modulation due to thermal deformation of grating in a spectral beam combining system, *Appl. Opt.* 56 (2017) 5511–5519.
- [14] S.A. Collins, Lens-systems diffraction integral written in terms of matrix optics, *J. Opt. Soc. Am.* 60 (1970) 1168–1177.
- [15] A. Belafhal, L. Dalil-Essakali, Collins formula and propagation of Bessel-modulated Gaussian light beams through an ABCD optical system, *Opt. Commun.* 177 (2000) 181–188.
- [16] D.R. Drachenberg, O. Andrusyak, G. Venus, V. Smirnov, L.B. Glebov, Thermal tuning of volume Bragg gratings for spectral beam combining of high-power fiber lasers, *Appl. Opt.* 53 (2014) 1242–1246.
- [17] J.W. Goodman, Introduction to Fourier Optics, Roberts & Company Publishers (2005).
- [18] A.E. Siegman, How to (maybe) measure laser beam quality, *Diode Pumped Solid State Lasers: Appl. Issues* 17 (1998) 184–199.
- [19] E.J. Bochove, Theory of spectral beam combining of fiber lasers, *IEEE J. Quantum Electron.* 38 (2002) 432–445.
- [20] Robert V. Hogg, Joseph McKean, Allen T. Craig, Introduction to Mathematical Statistics, seventh ed., Prentice Hall, 2012.

<sup>1</sup> For interpretation of color in Fig. 7, the reader is referred to the web version of this article.